Research Article

Different Effects of Mg^{2+} and Zn^{2+} on the Two Sites for Alkylammonium Compounds in *Pseudomonas aeruginosa* Phosphorylcholine Phosphatase

Lisandro Horacio Otero, Paola Rita Beassoni, Cristhian Boetsch, Angela Teresita Lisa, and Carlos Eduardo Domenech

Departamento de Biología Molecular, Facultad de Ciencias Exactas, Físico-Químicas y Naturales, Universidad Nacional de Río Cuarto, Ruta Nacional 36 Km 601, Río Cuarto, 5800 Córdoba, Argentina

Correspondence should be addressed to Carlos Eduardo Domenech, cdomenech@exa.unrc.edu.ar

Pseudomonas aeruginosa phosphorylcholine phosphatase (PchP) catalyzes the hydrolysis of phosphorylcholine (Pcho), is activated by Mg^{2+} or Zn^{2+}, and is inhibited by high concentrations of substrate. This study has shown that PchP contains two sites for alkylammonium compounds (AACs): one in the catalytic site near the metal ion-phosphoester pocket, and the other in an inhibitory site responsible for the binding of the alkylammonium moiety. The catalytic mechanism for the entry of Pcho in both sites and Zn^{2+} or Mg^{2+} follows a random sequential mechanism. However, Zn^{2+} is more effective than Mg^{2+} at alleviating the inhibition produced by the entry of Pcho or different AACs in the inhibitory site. We postulate that Zn^{2+} induces a conformational change in the active center that is communicated to the inhibitory site, producing a compact or closed structure. In contrast, Mg^{2+} produces a relaxed or open conformation.

1. Introduction

Pseudomonas aeruginosa phosphorylcholine phosphatase (PchP) catalyzes the hydrolysis of phosphorylcholine (Pcho) [1]. Pcho is the product of the action of hemolytic phospholipase C (PlcH) on phosphatidylcholine or sphingomyelin and is hydrolyzed to choline and inorganic phosphate (Pi) by the action of PchP. Thus, both the PlcH and PchP enzymes are involved in the pathogenesis of *P. aeruginosa* [2]. PchP contains three motifs that are characteristic of the enzymes belonging to the haloacid dehalogenase (HAD) superfamily [3]. Moreover, all three motifs have an important role in the catalytic process of Pcho or *p*-nitrophenylphosphate (*p*-NPP) in the presence of Mg^{2+}, Zn^{2+}, or Cu^{2+} as activators of the enzyme [4]. Using Pcho as the substrate, we have shown that Mg^{2+} is an equal activator for the enzyme at pH 5.0 and at pH 7.4; however, Zn^{2+} is an activator at pH 5.0 but an inhibitor at pH 7.4. The inhibition produced by Zn^{2+} at

pH 7.4 is reversible and occurs in the presence or absence of Mg^{2+}. This activation or inhibition of PchP by Zn^{2+} is caused by the transition from octahedral to tetrahedral geometry in the coordination sphere of the metal ion [5]. These results, in combination with the fact that PchP is inhibited by high Pcho concentrations and previous observations that different AACs may act as inhibitors of PchP [1, 6, 7], led us to evaluate the catalytic mechanism of PchP with Pcho as the substrate, Mg^{2+} or Zn^{2+} as activators, and AACs as inhibitors.

2. Materials and Methods

2.1. Materials. Isopropyl-β-D-thiogalactopyranoside (IPTG) and HisLink$^{\text{TM}}$ resin were purchased from Promega. Pcho and *p*-NPP were purchased from Sigma-Aldrich Co. Trimethylamine hydrochloride, tetramethylammonium chlo-ride (T4MA), choline chloride, chlorocholine chloride, betaine hydrochloride, hexamethonium chloride, decamethonium

bromide, tubocurarine hydrochloride pentahydrate, neostigmine bromide, 2-amino-2-methyl$-$1-propanol, L-histidinol dihydrochloride (Sigma-Aldrich), and all other chemicals were of analytical quality (Sigma-Aldrich or Merck).

2.2. Bacterial Strains, Growth Conditions, and Enzyme Purification.

The production of the PchP His-tag fusion protein in *E. coli* BL21 CodonPlus (Stratagene) was performed as previously described [5]. In the enzyme's purification, 1.5 mM de EDTA was added to remove any residual metal. Thereafter, the water utilized was three times distilled in glass and checked by Atomic Absorption Spectrometry (AAS). Under this condition, without the addition of metal ion, phosphorylcholine phosphatase activity was not found when it was measured in optimal conditions with Pcho or p-NPP as substrates. The addition of very low Zn^{2+} concentration, 0.5 μM, or 0.25 mM Mg^{2+} produced effective enzyme activation. The protein yield was between 15 mg L^{-1} and 20 mg L^{-1}. The specific activity, as measured with 10 mM p-NPP and 2 mM Mg^{2+}, was 110 μmoL p-nitrophenol min^{-1} (mg protein)$^{-1}$. The specific activity of the same preparation, as measured with 0.05 mM Pcho and 2 mM Mg^{2+}, was 54.5 μmoL Pi min^{-1}(mg protein)$^{-1}$.

2.3. Protein Concentration.

The protein concentration was determined by spectrophotometric measurement at 280 nm, using the theoretical molar extinction coefficient (ε = 69,915 M^{-1} cm^{-1}) [8]. Additional details have been described previously [5].

2.4. Enzyme Activity and Kinetic Data Analysis.

The standard assay to measure acid phosphatase activity was performed with p-NPP [4]. PchP activity with Pcho as the substrate was measured based on the release of Pi as described by Baykov et al. [9] and detailed by Otero et al. [5]. One unit of PchP was defined as the amount of enzyme that released 1 μmoL of p-nitrophenol or Pi from p-NPP or Pcho per minute at 37°C. Kinetic data were analyzed using the program DYNAFIT (http://www.biokin.com/dynafit) [10] to perform the global fits of the data to assess the best fit to activation and inhibition mechanisms (model discrimination analysis) and to calculate the corresponding constants. Results for Pcho inhibition of the enzyme activity, as measured with p-NPP, were analyzed utilizing the Hill equation: $\log v/V - v = K_{0.5} - n\log[I]$ as described previously [11].

2.5. Analysis of the Metal Ion-Ligand Distances.

Distances between the metal ion and ligands found in the active site of PchP were calculated with the program MESPEUS (http://tanna.bch.ed.ac.uk/) for metal coordination groups in proteins based on distances in the Cambridge Structural Database (*CSD*) and other data taken from protein structures determined at or near atomic resolution [12].

3. Results

3.1. PchP Activity with Pcho as Substrate and Mg^{2+} or Zn^{2+} as Activators.

The saturation curves of PchP with different Pcho concentrations in the presence of variable concentrations of Mg^{2+} or Zn^{2+} are shown in Figures 1(a) and 1(b), respectively. The kinetic constants, K_M and K_A, indicated that the K_M values for Pcho did not change in the presence of Mg^{2+} or Zn^{2+} despite the fact that Zn^{2+} has 1,000-fold stronger affinity for PchP compared to Mg^{2+} (Table 1). Comparison of the curves from Figures 1(a) and 1(b) demonstrates that the inhibition in the presence of Zn^{2+} produced by high Pcho concentrations significantly decreased as compared to the curves obtained in the presence of Mg^{2+}. The K_{SI} values for Pcho in the presence of Zn^{2+} were nearly 33-fold higher than the values obtained in the presence of Mg^{2+} (Table 1). These results led us to conduct experiments with p-NPP or Pcho as substrates with either T4MA or Pcho as inhibitors in the presence of Mg^{2+} or Zn^{2+}.

3.2. Inhibition by T4MA with p-NPP or Pcho as Substrates and Mg^{2+} or Zn^{2+} as Activators.

p-NPP was employed as the substrate to avoid interaction of the active site of PchP with the alkylammonium moiety, which is contained in the Pcho molecule. Consequently, the inhibition produced by T4MA was caused only by the NR_4^+ group of the AAC. The inhibition curves resulting from T4MA that were obtained in the presence of Mg^{2+} or Zn^2 indicated that Zn^{2+} was more effective than Mg^{2+} in preventing the inhibition produced by increasing concentrations of the T4MA (Figure 2 and Table 1).

The differential effect of Mg^{2+} and Zn^{2+} on the inhibition caused by T4MA was also observed by measuring the enzyme activity with subinhibitory concentrations of Pcho as substrate (Figure 3). Under these conditions and in the presence of Mg^{2+}, the inhibition produced by increasing concentrations of Pcho and variable T4MA concentrations had an additive effect (Figure 3(a)). In contrast, the inhibition produced by increasing concentrations of both AACs in the presence of Zn^{2+} was low or nearly negligible (Figure 3(b)).

3.3. Inhibition of PchP by Pcho with p-NPP as Substrate and Mg^{2+} or Zn^{2+} as Activators.

The inhibitory effect of Pcho on PchP activity when the activity was measured with p-NPP as the substrate and Mg^{2+} or Zn^{2+} as activators is shown in Figure 4. The "n" Hill coefficient value decreased from 1.8 in the presence of Mg^{2+} to 1.2 in the presence of Zn^{2+} (Table 1).

3.4. AACs as Inhibitors of PchP.

The PchP activity measured with variable concentrations of p-NPP and variable concentrations of AAC in the presence of Mg^{2+} indicated that all of the tested AACs were inhibitors of PchP with different degrees of efficiency (Table 2). At 1 mM final concentration, the highest percentages of inhibition were produced by trimethylamine, T4MA, choline, chlorocholine, hexamethonium, and decamethonium. This inhibition was also reflected in the low values of the K_I1 and K_I2 constants. To a lesser extent, 2-amino-2-methyl$-$1-propanol and L-histidinol, which are compounds with an N-positive charge but without methyl groups attached to the nitrogen atom, were also poor inhibitors of enzyme activity (Table 2). In addition to the presence of a charged group, such as the
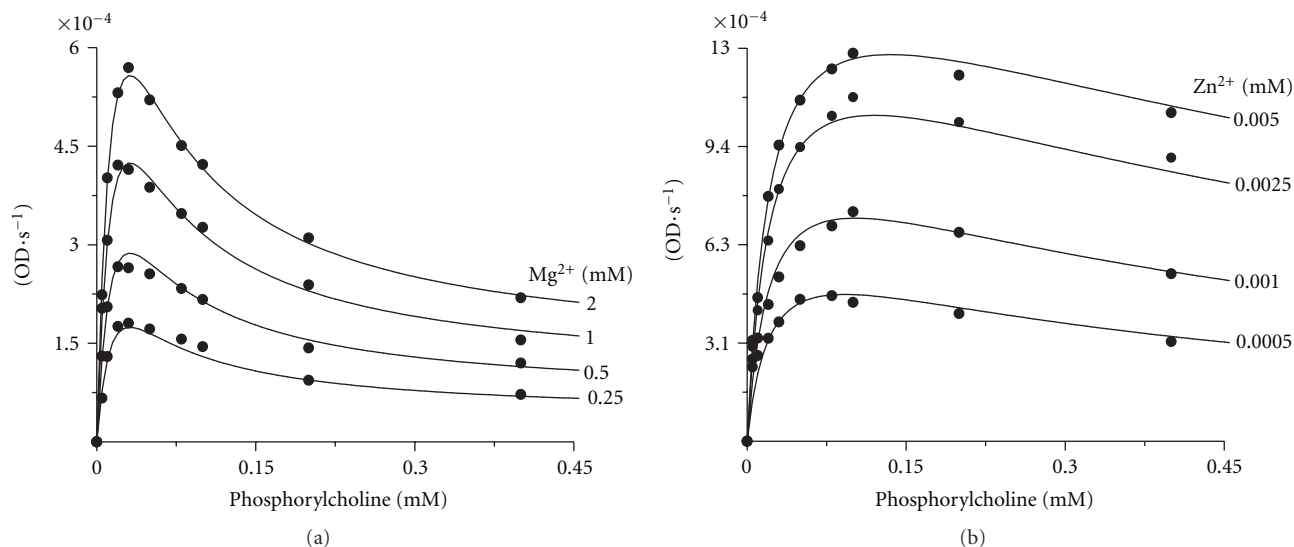
(a)

(b)

FIGURE 1: Saturation curves for PchP with different Pcho concentrations (0.0005–0.4 mM) in the presence of 0.25 mM, 0.5 mM, 1 mM, and 2 mM Mg^{2+} (a) or 0.0005 mM, 0.001 mM, 0.0025 mM, and 0.005 mM Zn^{2+} (b). The enzyme activity was measured in 100 mM sodium acetate buffer, pH 5.0. The statistics of least-squares fit were as follows: mean square = 9.99254×10^{-11} (a) and 1.08357×10^{-9} (b); root-mean-square deviation = 9.99627×10^{-6} (a) and 3.29177×10^{-5} (b); number of datapoints = 40; optimized parameters = 6; degrees of freedom = 34; percentage confidence interval level = 99%.
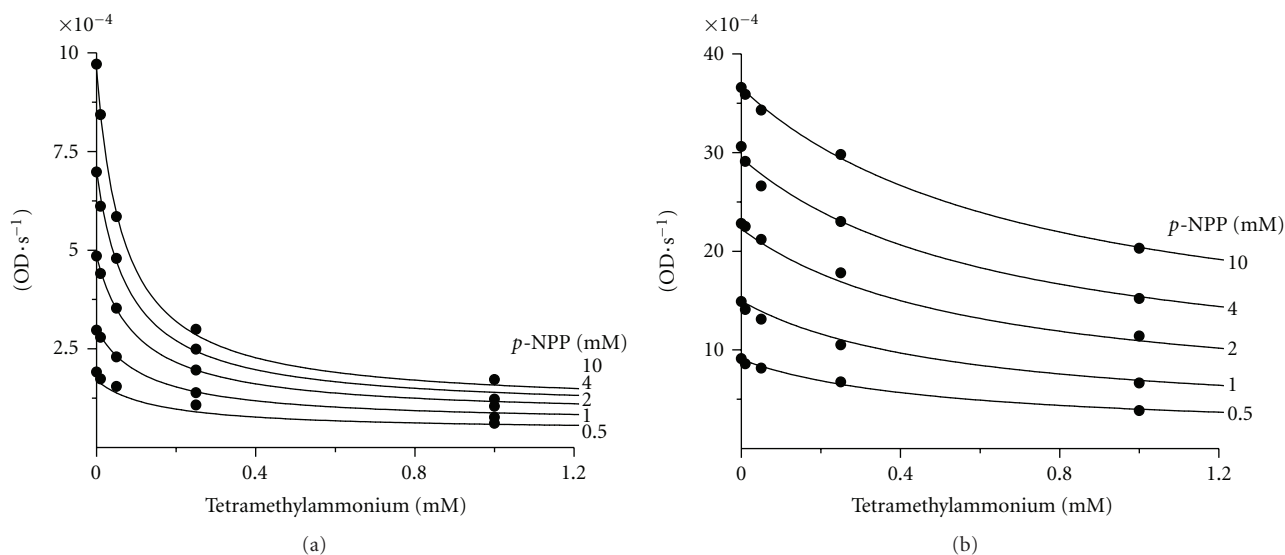

(a)

(b)

FIGURE 2: Inhibition of PchP activity by T4MA in the presence of 2 mM Mg^{2+} (a) or 0.03 mM Zn^{2+} (b). The enzyme activity was measured with different p-NPP concentrations (0.5 mM, 1 mM, 2 mM, 4 mM, and 10 mM) in 100 mM sodium acetate buffer, pH 5.0. The statistics of least-squares fit were as follows: mean square = 1.26295×10^{-10} (a) and 2.63174×10^{-9} (b); root-mean-square deviation = 1.12381×10^{-5} (a) and 5.13005×10^{-5} (b); number of datapoints = 24; optimized parameters = 5; degrees of freedom = 20; percentage confidence interval level = 99%.

$-COO^-$ in betaine, the presence of large-R groups, such as in neostigmine, or the decrease of N-methyl groups, such as in tubocurarine, also significantly reduced the inhibition of PchP, as shown by the comparison of K_I values or percentage of inhibition in Table 2.

4. Discussion

In this study, the experimental data treated with DYNAFIT resulted in two schemes for the PchP catalytic mechanism. Scheme 1 illustrates that (i) PchP binds two substrate

TABLE 1: Kinetic constants of PchP for substrate and inhibitors obtained in the presence of Mg^{2+} or Zn^{2+} as metal ion activators. Values $\pm$ SD of at least three experiments in duplicate were performed for each set of curves that are shown in each corresponding figure indicated in this table.

| Constants	Mg^{2+}	Zn^{2+}	Observations
K_{MPcho}, mM $\pm$ SD	0.021 ± 0.008	0.022 ± 0.007	Data taken from Figure 1 and Scheme 1
K_A, mM $\pm$ SD	0.91 ± 0.08	0.0009 ± 0.00005	
$k_{cat}1$, s$^{-1}\pm$ SD	121 ± 8	143 ± 12	
$k_{cat}2$, s$^{-1}\pm$ SD	12 ± 0.9	9 ± 0.7	
$K_{SI}1$, mM $\pm$ SD	ND	ND	$S \cdot E \cdot S$, Scheme 1, is a nonproductive complex
$K_{SI}2$, mM $\pm$ SD	0.037 ± 0.01	1.21 ± 0.09	Data taken from Figure 1 and Scheme 1
K_I1, mM $\pm$ SD	0.17 ± 0.04	0.83 ± 0.06	Data taken from Figure 2 and Scheme 2
K_I2, mM $\pm$ SD	0.035 ± 0.008	0.45 ± 0.07	
$K_{0.5}$, mM $\pm$ SD	0.056 ± 0.007	0.11 ± 0.02	Data taken from Figure 4
n Hill$_{value}\pm$ SD	1.8 ± 0.03	1.2 ± 0.08	

(a)

(b)
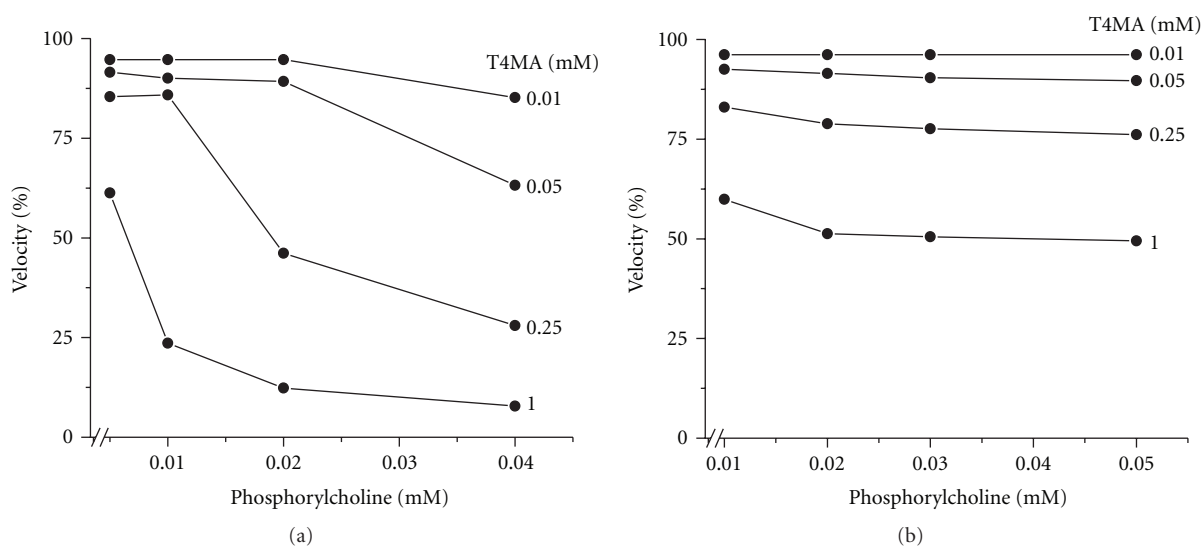
FIGURE 3: Effect of T4MA on the PchP activity measured at low Pcho concentrations. Pcho concentration varied between 0.005 mM and 0.04 mM when the activity was measured in the presence of 3 mM Mg^{2+}. With 0.003 mM Zn^{2+} as the activator, the Pcho concentration varied between 0.01 mM and 0.05 mM. As was shown in Figure 1, in these assay conditions there was no enzyme inhibition by high substrate concentrations. 3 mM Mg^{2+} and 0.003 mM Zn^{2+} correspond to three times the K_A values that are shown in Table 1. All determinations were performed in 100 mM sodium acetate buffer, pH 5.0. Because several parts of these experiments were performed with low Pcho concentrations, special care was taken to measure the enzyme activity under strict conditions of initial velocity.

molecules and one metal ion and (ii) the more probable mechanism for the catalytic action of PchP with Pcho is independent of the identity of the metal ion. Considering the first part of Scheme 1 (top), the kinetic parameters are consistent with a random sequential mechanism in which the metal ion (A) or the substrate (S) initially binds to PchP (E). The EA or ES complexes bind to S or A, respectively, to form the EAS productive complex before the enzyme releases the product (P). The second part of Scheme 1 (bottom) shows a random mechanism for the interaction of a second substrate molecule with the ES or EAS complexes to form SES or SEAS complexes (S before E in SES or in SEAS complexes indicates that the second Pcho molecule binds to a site different from the catalytic site of PchP). After SES binds, the metal ion also forms the SEAS complex, which is capable of forming P but does so with less efficiency than

the EAS complex. An interesting comparison can be made between the catalytic mechanisms resulting from the use of the two different substrates, Pcho and p-NPP. Using p-NPP as the substrate, an ordered mechanism occurs in the presence of Mg^{2+} or Zn^{2+} [4]. The discrepancy between the catalytic mechanisms may be caused by the different affinity of PchP for the substrates; one of the them is positively charged with an N-trimethylammonium moiety ($K_{MPcho} \approx$ 0.020 mM), and the other contains a p-nitrophenol group ($K_{M\,p\text{-NPP}} \approx 3$ mM). This difference in affinities may lead to a more equal competition between the metal and substrate for the enzyme because the presence of metal is not required for Pcho binding.

Experiments performed with Mg^{2+} or Zn^{2+} indicate that Zn^{2+} produced enzyme activation at concentrations 1,000-fold lower than Mg^{2+}, and Zn^{2+} prevented inhibition due

TABLE 2: Inhibition of PchP by AACs. Percentage inhibition was measured with 1 mM inhibitor, 10 mM p-NPP, and 2 mM Mg^{2+} at pH 5.0. Inhibition constants were calculated with the application of the program DYNAFIT from activity curves performed in the presence of 0.5, 1, 2, 4, and 10 mM p-NPP with 2 mM Mg^{2+} in 100 mM sodium acetate buffer, pH 5.0. The AAC concentrations were 0.01, 0.05, 0.25, and 1 mM. Values shown are averaged from three independent experiments ± SD. PU: partial uncompetitive and C: competitive inhibition.

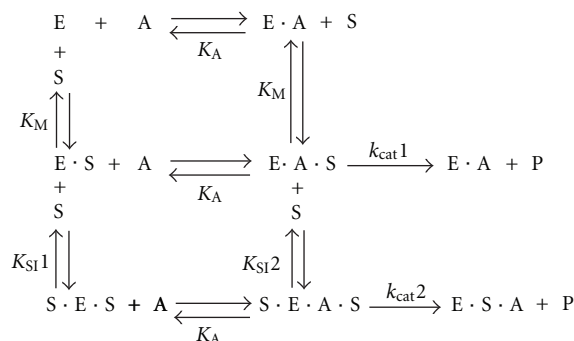| Inhibitor	Number of N-alkyl groups	% Inhibition	Inhibition constants		Type of inhibition
			K_I1, mM ± SD	K_I2, mM ± SD	
Trimethylamine	N,N,N-trimethyl	81	0.21 ± 0.03	0.06 ± 0.01	PU + C
Tetramethylammonium	N,N,N,N-tetramethyl	91	0.17 ± 0.04	0.04 ± 0.01	PU + C
Choline	1 N,N,N-trimethyl	85	0.89 ± 0.08	0.10 ± 0.01	PU + C
Chlorocholine	1 N,N,N-trimethyl	82	0.44 ± 0.04	0.12 ± 0.01	PU + C
Betaine	1 N,N,N-trimethyl	26	1.44 ± 0.09	7.75 ± 0.91	PU + C
Hexamethonium	2 N,N,N-trimethyl	85	0.37 ± 0.05	0.08 ± 0.01	PU + C
Decamethonium	2 N,N,N-trimethyl	83	0.21 ± 0.04	0.08 ± 0.01	PU + C
Tubocurarine	1 N-methyl + 1 N,N-dimethyl	22	2.51 ± 0.21	4.10 ± 1.20	PU + C
Neostigmine	1 N,N-dimethyl + 1 N,N,N-trimethyl	55	6.25 ± 0.34	0.57 ± 0.05	PU + C
2-amino-2-methyl-1-propanol	1 N	74	3.94 ± 0.16	0.21 ± 0.01	PU + C
L-histidinol	1 N	56	2.11 ± 0.05	0.31 ± 0.08	PU + C
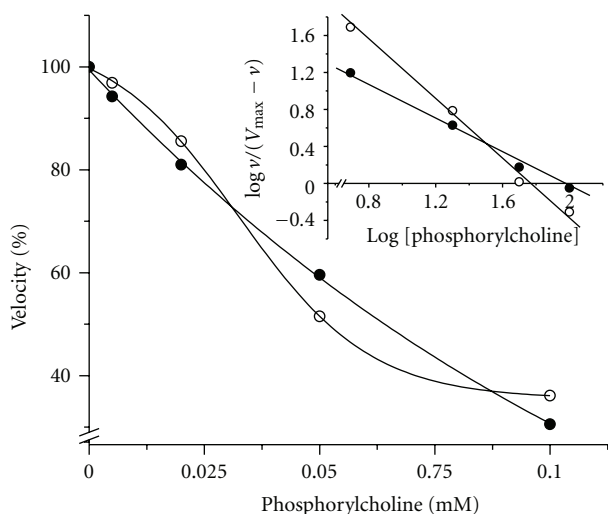
FIGURE 4: Inhibition of PchP activity by Pcho measured with 10 mM p-NPP in the presence of 2 mM Mg^{2+} (○) or 0.03 mM Zn^{2+} (●). All determinations were performed in 100 mM sodium acetate buffer, pH 5.0.

SCHEME 1: Catalytic mechanism of PchP with Pcho as substrate. The data shown in Figure 1 were analyzed with the program DYNAFIT. E: enzyme; S: substrate, Pcho; A: divalent cation activator; P: product.
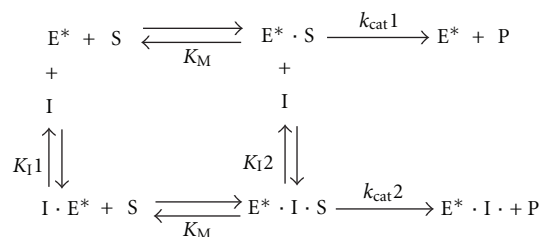
SCHEME 2: Mechanism of PchP inhibition produced by T4MA. The data shown in Figure 2 were analyzed with the program DYNAFIT. In this scheme, (E^*) represents the enzyme bound to the metal ion for simplicity. S: substrate, I: inhibitor, and P: product. In this scheme, $k_{cat}1 \gg k_{cat}2$.

to the entry of the second Pcho molecule much more effectively than Mg^{2+}. The experimental data obtained with T4MA showed that in the presence of either metal ion, Mg^{2+} or Zn^{2+}, the inhibition produced by T4MA followed a mixed-type inhibition mechanism with competitive and partial uncompetitive components (Scheme 2). This type of inhibition was obtained with p-NPP, which is a substrate without the alkylammonium moiety, and it is confirmatory that the enzyme contains two binding sites for alkylammonium ion: one site, which is indicated by the competitive component, may be the site for the alkylammonium moiety of the Pcho substrate, and the second site may be responsible for inhibition due to high substrate concentration, which was shown with Pcho.

Experiments with many AACs demonstrating competitive and uncompetitive inhibitory components and the clear differences found for the K_I1 and K_I2 values confirmed that PchP contains two binding sites for the alkylammonium moiety of Pcho. Among these compounds, the K_I1 and K_I2 values, as defined in Scheme 2, indicated that T4MA and trimethylamine were the compounds that possessed higher affinities for both alkylammonium sites of PchP. Based on the differences in the inhibitory capacity produced by the remaining AACs, the lowered inhibition and increased K_I values were caused by one or more of the following reasons: hydrophilic interactions, repulsion or attraction of charges, length or size of the molecule's structure, and lack of hydrophobic interactions at the opposing end of the inhibitory molecule. The importance of the number of N-methyl groups and the presence of hydroxyl or carboxyl groups in the structure of the inhibitory molecule has been previously discussed [7]. Overall, the kinetic data suggest that *P. aeruginosa* PchP contains a catalytic site with an inhibitory site in its vicinity. The catalytic site is formed by two subsites: one subsite is for the phosphoester moiety of Pcho, which is closely associated with the metal ion site, and the second subsite is responsible for the binding of the N-trimethyl moiety of Pcho. The inhibitory site also has the capacity to bind the N-trimethyl moiety of Pcho.

The most notable result from this study was the differential effects of Zn^{2+} and Mg^{2+} as activators of PchP when the enzyme was in the presence of high concentrations of Pcho or T4MA. According to Beassoni et al. [4] and Otero et al. [5], the octahedral coordination complex between Mg^{2+} or Zn^{2+} with different ligands is formed with the carboxylate groups of ^{31}D and ^{262}D, the carbonyl group of ^{33}D, the oxygen from the phosphate and two water molecules. Therefore, to explain the differential effect of Zn^{2+} and Mg^{2+}, we believe that it is necessary to consider the fact that $^{65}_{30}Zn$ has a higher nuclear charge than $^{24}_{12}Mg$. The consequence of this different nuclear charge may be translated into changes in bond distances between the central metal ion and the different functional groups of the enzyme that are coordinately involved to form the octahedral complex with Mg^{2+} or Zn^{2+}. This assumption may be supported by considering the distances that were calculated with the MESPEUS program when assigning the coordination index for Mg^{2+} and Zn^{2+} to be six. The average distances between Mg^{2+} and the $-COO^-$ and C=O groups were 2.07 Å and 2.26 Å, respectively. Shorter average distances were obtained for Zn^{2+}, $-COO^-$ and C=O groups at 1.99 Å and 2.07 Å, respectively. If these average distances are present in the coordination compounds formed from the active site residues of PchP and the two metal ions, it is possible to assume that the coordination sphere of the octahedral complex forms an open or relaxed active center in the presence of Mg^{2+}, whereas the presence of Zn^{2+} shifts the conformation of the active center toward a closed or compact form. This conformational change may not be a stochastic process but is a process directed by the interaction forces produced by the higher nuclear charge of the Zn^{2+} ions as compared to the nuclear charge of the Mg^{2+} ions. Therefore, it is reasonable to postulate that Zn^{2+} induces a conformational change as proposed by Weikl and Von Deuster [13], which may promote the hydrolysis of Pcho and decrease its inhibitory effect by preventing the entry of the second substrate molecule.

From a physiological standpoint, it is interesting to note that the activity of this enzyme is controlled by environmental factors, such as N-methylammonium compounds, Mg^{2+} and Zn^{2+} that are present or may be found in any ecological niche, where *P. aeruginosa* can grow and multiply. Considering that the infectious process takes place in an acidic medium, where *P. aeruginosa* can find free Pcho or esterified phosphatidylcholine or sphingomyelin, our present data in addition to those described previously [5] indicate that, at low concentrations, Zn^{2+} favors the action of PchP to release choline through two processes: (i) by increasing its catalytic activity at low concentrations of substrate and (ii) by its protective effect against enzyme inhibition that may be caused by high concentrations of Pcho or other AACs.

We have recently crystallized PchP and obtained preliminary X-ray diffraction data for the enzyme [14]. Thus, we will be able to investigate the interactions of the enzyme with substrate, metal ions, and other effectors in more detail based on the solved structure of PchP in the near future, and we will be able to gain very useful information on the relationship between the structure and function of this enzyme in greater depth.
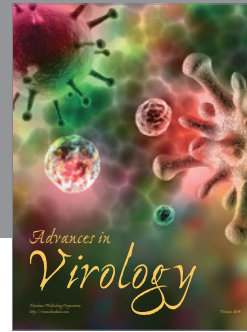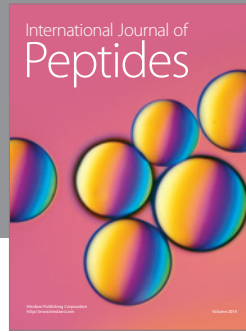
Acknowledgments

References

[1] M. A. Salvano and C. E. Domenech, "Kinetic properties of purified *Pseudomonas aeruginosa* phosphorylcholine phosphatase indicated that this enzyme may be utilized by the bacteria to colonize in different environments," *Current Microbiology*, vol. 39, no. 1, pp. 1–8, 1999.

[2] A. T. Lisa, P. R. Beassoni, M. J. Masssimelli, L. H. Otero, and C. E. Domenech, "A glance on *Pseudomonas aeruginosa* phosphorylcholine phosphatase, an enzyme whose synthesis depends on the presence of choline in its environment," in *Communicating Current Research and Educational Topics and Trends in Applied Microbiology*, pp. 255–262, Badajoz, Spain, 2007.

[3] P. R. Beassoni, L. H. Otero, M. J. Massimelli, A. T. Lisa, and C. E. Domenech, "Critical active-site residues identified by site-directed mutagenesis in *Pseudomonas aeruginosa* phosphorylcholine phosphatase, a new member of the haloacid dehalogenases hydrolase superfamily," *Current Microbiology*, vol. 53, no. 6, pp. 534–539, 2006.

[4] P. R. Beassoni, L. H. Otero, A. T. Lisa, and C. E. Domenech, "Using a molecular model and kinetic experiments in the presence of divalent cations to study the active site and catalysis of *Pseudomonas aeruginosa* phosphorylcholine phosphatase," *Biochimica et Biophysica Acta*, vol. 1784, no. 12, pp. 2038–2044, 2008.

[5] L. H. Otero, P. R. Beassoni, A. T. Lisa, and C. E. Domenech, "Transition from octahedral to tetrahedral geometry causes the activation or inhibition by Zn^{2+} of *Pseudomonas aeruginosa* phosphorylcholine phosphatase," *BioMetals*, vol. 23, no. 2, pp. 307–314, 2010.

[6] T. A. Lisa, M. N. Garrido, and C. E. Domenech, "*Pseudomonas aeruginosa* acid phosphatase and cholinesterase induced by choline and its metabolic derivatives may contain a similar anionic peripheral site," *Molecular and Cellular Biochemistry*, vol. 63, no. 2, pp. 113–118, 1984.

[7] M. N. Garrido, T. A. Lisa, and C. E. Domenech, "*Pseudomonas aeruginosa* acid phosphatase contains an anionic site with a trimethyl subsite—kinetic evidences obtained with alkylammonium ions," *Molecular and Cellular Biochemistry*, vol. 84, no. 1, pp. 41–49, 1988.

[8] E. Gasteiger, C. Hoogland, A. Gattiker et al., "Protein identification and analysis tools on the ExPASy server," in *The Proteomics Protocols Handbook*, pp. 571–607, Humana Press Inc., Totowa, NJ, USA, 2005.

[9] A. A. Baykov, O. A. Evtushenko, and S. M. Avaeva, "A malachite green procedure for orthophosphate determination and its use in alkaline phosphatase-based enzyme immunoassay," *Analytical Biochemistry*, vol. 171, no. 2, pp. 266–270, 1988.

[10] P. Kuzmič, "Program DYNAFIT for the analysis of enzyme kinetic data: application to HIV proteinase," *Analytical Biochemistry*, vol. 237, no. 2, pp. 260–273, 1996.

[11] I. H. Segel, "Behavior and analysis of rapid equilibrium and steady-state enzyme systems," in *Enzyme Kinetics*, John Wiley and Sons, New York, NY, USA, 1975.

[12] K. Hsin, Y. Sheng, M. M. Harding, P. Taylor, and M. D. Walkinshaw, "MESPEUS: a database of the geometry of metal sites in proteins," *Journal of Applied Crystallography*, vol. 41, no. 5, pp. 963–968, 2008.

[13] T. R. Weikl and C. Von Deuster, "Selected-fit versus induced-fit protein binding: kinetic differences and mutational analysis," *Proteins*, vol. 75, no. 1, pp. 104–110, 2009.

[14] L. H. Otero, P. R. Beassoni, C. E. Domenech, A. T. Lisa, and A. Albert, "Crystallization and preliminary X-ray diffraction analysis of *Pseudomonas aeruginosa* phosphorylcholine phosphatase," *Acta Crystallographica Section F*, vol. 66, no. 8, pp. 957–960, 2010.

BioMed
Research International

Stem Cells
International

International Journal of
Peptides

Advances in
VIROLOGY

International Journal of
Genomics

International Journal of
Zoology

Journal of
Nucleic Acids

Journal of
Signal Transduction

Hindawi

Submit your manuscripts at
http://www.hindawi.com

The Scientific
World Journal

Genetics
Research International

Anatomy
Research International

International Journal of
Microbiology

Biochemistry
Research International

Advances in
Bioinformatics

Archaea

Enzyme
Research

International Journal of
Evolutionary Biology

Molecular Biology
International

Journal of
Marine Biology